Chapter 4

Incorporation of first-order backscattered power in Water Cloud Model for improving the Leaf Area Index and Soil Moisture retrieval using dual-polarized Sentinel-1 SAR data

4.1 Introduction

Information on vegetation characteristics is important to assess crop growth and health (Bhogapurapu et al., 2021; Dabrowska-Zielinska et al., 2007; Verma et al., 2022). The retrieval of this information over a large landscape is essential to validate models and evaluate net productivity, biosphere-atmosphere exchange of heat, and other vegetation-atmosphere properties. Among many vegetation attributes, some of the most important include LAI, Vegetation Water Content (VWC), plant height (h), and biomass. The LAI, in

particular, is a dimensionless parameter defined as the projected area of leaves over a unit area of land (m^2m^{-2}) (Bréda, 2008; Kalácska et al., 2005; Price, 1993; Singh et al., 2022). It is a key indicator of vegetation growth and productivity and can be estimated through direct (field sampling) and indirect (remotely sensed satellite data) methods. However, direct methods of LAI estimation can be time-consuming and cumbersome, making non-destructive indirect methods more favorable for extensive landscape observations (Garcia-Haro et al., 1996; Turner et al., 1999). Remote sensing, utilizing both optical and microwave frequencies, can provide vital information on the surface and atmosphere of the Earth. Microwave remote sensing has some advantages over optical remote sensing, as it can penetrate through clouds, smoke, and vegetation and provide all-weather imaging capability. This makes microwave remote sensing useful for applications such as mapping soil moisture content, measuring sea ice thickness, and monitoring the Earth's water cycle.

Several studies have used satellite SAR time series data (Sentinel-1, RADARSAT, ALOS) to derive the vegetation descriptor and biophysical parameters (Kim and Van Zyl, 2009; Li et al., 2021; Mandal et al., 2020; Periasamy, 2018). SAR incidence angle, polarization, and operating frequency play a significant role in the observation of the topographical and morphological features of the Earth. The backscattering coefficient measured by SAR sensors provides information about the surface properties and vegetation, and the response to these factors is dependent on the incidence angle of the radar wave (Autret et al., 1989; Wang et al., 1993; Yadav et al., 2022a; Zribi et al., 2014). A lower incidence angles in SAR imaging are better suited for soil properties retrieval, while higher incidence angles are more sensitive to the canopy and its properties (Sun et al., 1991; Ulaby et al., 1982; Wang et al., 1993). Thus, an optimal incidence angle is required for vegetation and surface studies. Also, the different polarization of microwave electromagnetic signals interacts differently with surface and vegetation. To get a good response from the vegetation and soil surface right choice of polarization is essential. Various studies extensively

covered the sensitivity of different polarizations with different surfaces; for example, VV polarization is more sensitive to soil moisture than HH due to better responsiveness to variations in surface roughness and dielectric properties of the soil, caused by moisture content (Autret et al., 1989; Singh et al., 1996; Zeng and Chen, 2018). However, it has been found that cross-polarized SAR imagery manifested great sensitivity towards the vegetation layers which suggests that to some extent, the sensitivity of cross-polarized SAR depends upon the structure and pattern of the vegetation (Holah et al., 2005; Li et al., 2014; Mandal et al., 2020).

The estimation of vegetation properties (canopy structure, biomass, and VWC) and soil properties (soil moisture, dielectric constant, and roughness parameter) can be challenging using SAR data. Remote sensing scattering models cannot directly be applied to SAR or optical data to determine soil or vegetation properties. The estimation of soil properties and vegetation properties using remote sensing data is a complex process because vegetation contains water content, which can interact with electromagnetic radiation and affect the scattering phenomenon. The water content in vegetation can change the dielectric properties of the vegetation, leading to variations in the scattering and absorption of the SAR signal. The wavelength dependency of the radar signal can also affect the scattering mechanisms that are responsible for the radar backscatter from the soil and vegetation, further complicating the process of separating the contributions from each layer (Bindlish and Barros, 2001; Dobson and Ulaby, 1986; Zribi et al., 2007). For example, longer wavelength SAR systems, such as L-band and P-band, have a greater penetration capability but may provide less detailed information about the vegetation canopy, while shorter wavelength SAR systems, such as X-band and C-band, have a higher resolution, but may have more difficulty penetrating through the canopy. Currently, researchers are focused on separating scattering phenomena from different bodies, mainly in two ways. The first is the polarization decomposition method, which utilizes the different polarizations (vertical,

horizontal, circular) of the electromagnetic signal to separate the scattering from different surfaces (An et al., 2010; Freeman and Durden, 1998; Yamaguchi et al., 2005). The second approach is based on scattering models, which use mathematical equations to simulate the scattering process and estimate the properties of the surface layers. For scattering models, the widely used model is the Water Cloud Model (WCM) (Attema and Ulaby, 1978). It is a semi-empirical model that simplifies the complex scattering between surface and vegetation layers. Another model is the Michigan Microwave Canopy Scattering (MIMICS) model proposed by Ulaby(Ulaby et al., 1990), which is a physical model that can be used to study the vegetation and soil surface layer. However, the complexity and the high number of input variables in the model make it less practical than the WCM.

In WCM, it is believed that the vegetative layer is a homogenous layer of water cloud droplets. In other words, a uniform medium and a descriptor are used to define this vegetation layer's properties. The WCM is relatively less complex and computationally less expensive than the other models for example RTM and the FDTD (Finite Difference Time Domain). The inclusion of different soil backscattering models in conjunction with WCM helped to retrieve vegetation and soil parameters accurately and are categorized as physical, semi-empirical, and empirical (Bai and He, 2015; Yadav et al., 2022b; Zribi et al., 2005). A previous study conducted an evaluation of the Oh model and the Integral Equation Model (IEM) using SAR data at L-, C-, and X-bands, in conjunction with in situ measurements. The results of their analysis revealed that the IEM provided accurate simulations, with Root Mean Square Error (RMSE) values of approximately 2.0 dB, primarily when applied to smooth surfaces. Conversely, when applied to rough surfaces and at medium incidence angles, the Oh model simulations were found to yield backscattering values that were in close agreement with the measured values (Baghdadi et al., 2011; Choker et al., 2017; Panciera et al., 2013). However, an empirical model like Dubois's is easy to use due to its less complicated nature, but its data and site dependency make it limited in applications

(Dubois et al., 1995; Zribi et al., 2005). The semi-empirical such as the Oh model for the soil surface backscattering, utilize a physical background and incorporates simulated and empirical observations to make the models more tractable and easier to use in practice (Attema and Ulaby, 1978; Oh, 2004; Oh et al., 1992).

However, due to non-homogeneity in the stretch of the large landscape, the parameterization of the simplified model is the key issue in the practical implementation of WCM. The WCM attempts to use straightforward vegetation parameters to represent the canopy scattering and attenuation components in the model. The literature has employed a number of bulk factors as vegetation descriptors, such as plant water content, biomass, LAI, and VWC (Park et al., 2019; Verma et al., 2022). However, there hasn't been much research on picking the best vegetation descriptors for the WCM. Furthermore, the WCM ignores the mutually influencing interaction between plant and soil surfaces, which has a substantial influence on the total scattering and attenuation properties of the land surface. The WCM model assumes two independent contributions from plant and soil surfaces, without taking into account their interactions. When the plant density is considerable, this might cause a large departure from the true scattering and attenuation properties of the ground surface. This can be called the "vegetation-soil interaction effect," and it is an essential component to consider when parameterizing the WCM model. In this paper, a novel modification to the traditional Water Cloud Model (WCM) called the modified WCM (mWCM) is proposed, aimed at improving LAI and SM retrieval using Sentinel-1 SAR datasets for wheat crops. The main contribution to the modification came from the incorporation of scaling constants for vegetation, soil, and vegetation-soil interaction within the WCM, as well as the integration of a first-order scattering component from the Vegetation-Soil Scattering Model (VSSM). The methodology includes accurate simulation of the total backscattering and account for the combined effect of vegetation and soil surface layer. The proposed work is organized in a methodical and systematic manner as follows: In section 2, the study

area and the field measurements conducted, along with the pre-processed dual-polarized Sentinel-1 SAR datasets utilized in the study, are described in detail. In section 3, the proposed methodology of the modified Water Cloud Model (mWCM) is presented. The methodology encompasses the derivation of novel scaling factors via the utilization of a covariance matrix, which is then employed to formulate the Vegetation-Soil Scattering Model (VSSM). Subsequently, the VSSM is integrated within the mWCM to simulate the total backscattering coefficients for a wheat crop. In section 4, various statistical indices such as coefficients of determination (R^2), Root Mean Square Error (RMSE), and Nash Sutcliffe Efficiency (NSE) are employed to evaluate the performance of the scattering model and retrieval. In section 5, the sensitivity analysis of the mWCM is presented. In section 6, the implementation of the mWCM algorithm is discussed in depth, and the simulation and retrieval performance of the mWCM are rigorously evaluated. Finally, in section 7, the proposed work is succinctly summarized and conclusions are drawn.

4.2 Study area and data used

4.2.1 Study area

This study is conducted in the Gangetic plain region of Varanasi district, located in the northern state of India (Figure 4.1). The region is selected for its distinct agro-climatic characteristics, specifically its longitude and latitude of 82°58′56.92″ E and 25°15′55.27″ N respectively. The area is characterized by its annual precipitation patterns, with a majority of the rainfall occurring during the monsoonal season, typically from July to September, and a total annual precipitation of approximately 1110 mm. Additionally, the region exhibits a wide range of temperature variations, ranging from 9 °C to 42 °C throughout the year. The region is also known for its alluvial soil deposits, which are highly fertile, making it an ideal location for agriculture.

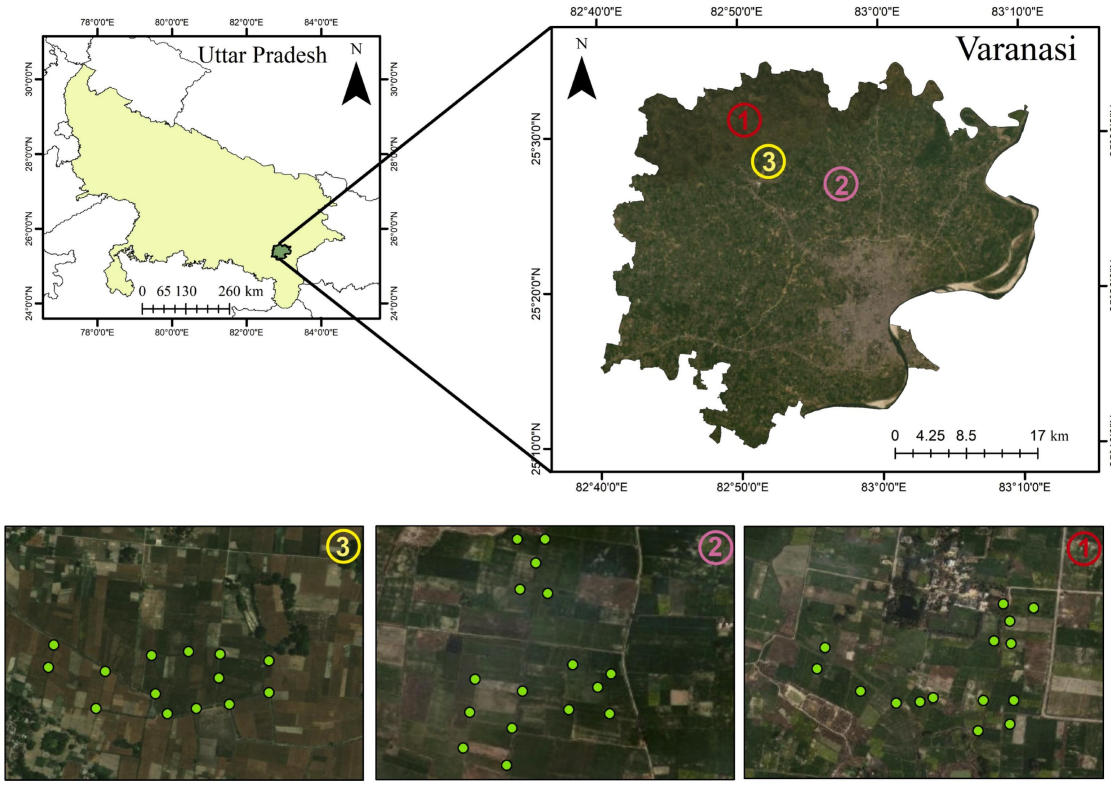

Figure 4.1 Study area showcasing locations (comprising location 1 in red 2 in pink and 3 in yellow) with sampling points, providing a comprehensive view of the entire study region.

4.2.2 Field data observation

In this study, in situ measurements are conducted on three reference fields of varying sizes ranging from 3 to 5 km^2, in conjunction with a SAR data acquisition date. The primary objective of the in-situ measurements is to gather data on LAI using the Li-Cor measurement device, with the utmost care taken to ensure proper calibration and the absence of any contamination in the obtained measurements. The mean of three readings was taken for each LAI measurement.

In addition to LAI, soil moisture, and surface roughness are also measured utilizing the HydraGo device (Figure 4.2(a)) and a one-meter-long metallic plate painted with the grid of an area of 1 cm square (Figure 4.2(b)) respectively. The SM measurements are taken from a depth of 2–5 cm, with a mean of 2–3 measurements taken at each point. The surface

roughness measurements are performed by inserting the metallic plate into the surface until the grid lines reach the lowest point. The digitization of the roughness profile was then carried out for the calculation of the root mean square (RMS) height and correlation length. The RMS height is a statistical measure of the surface roughness and it was calculated by measuring the vertical deviation of each point of the roughness profile from the mean value and taking the square root of the mean of the squares of these deviations.

(a) (b)

Figure 4.2 The procedure of measuring (a) soil moisture using HydraGO, (b) surface roughness profile.

The collected data was from three distinct reference fields (Table 4.1), where the number of samples was nearly equal from each field. To ensure unbiased results, we used the datasets from the first and second fields for training the mWCM and reserved the dataset from the third field for validation. We made sure of a 70:30 (2 field: 1 field) ratio for this purpose, with 70% of the pooled data being used for training and the other 30% for validation (Nguyen et al., 2021; Saha et al., 2021). It is worth noting that this division of the data set ensures that the mWCM is well-trained and at the same time the validation dataset is independent, providing an unbiased evaluation of the model's performance.

Figure 4.3 illustrates the temporal variations of observed LAI and soil moisture over the winter. In the early days of crop sowing, when growth was minimal, LAI was recorded low, and as the growing season progressed, LAI increased and reached its peak in March. The database covering 5 dates included the entire phenological stages of the crop in the study region. A rise in soil moisture variation was recorded on January 25 as a result of irrigation. Except for this, the soil moisture variation was subtle throughout the study.

Table 4.1 Summary of in-situ measurements collected from three reference fields.

Location	LAI (m2/m2) (min-max)	SM (m3/m3) (min-max)	Sampling point	Sampling date
Location-1	0.56–4.8	0.16–0.40	67	03/01/2020, 25/01/2020
Location-2	1.08–5.58	0.12–0.41	68	07/02/2020, 23/02/2020
Location-3	0.98–6.21	0.14–0.38	65	05/03/2020

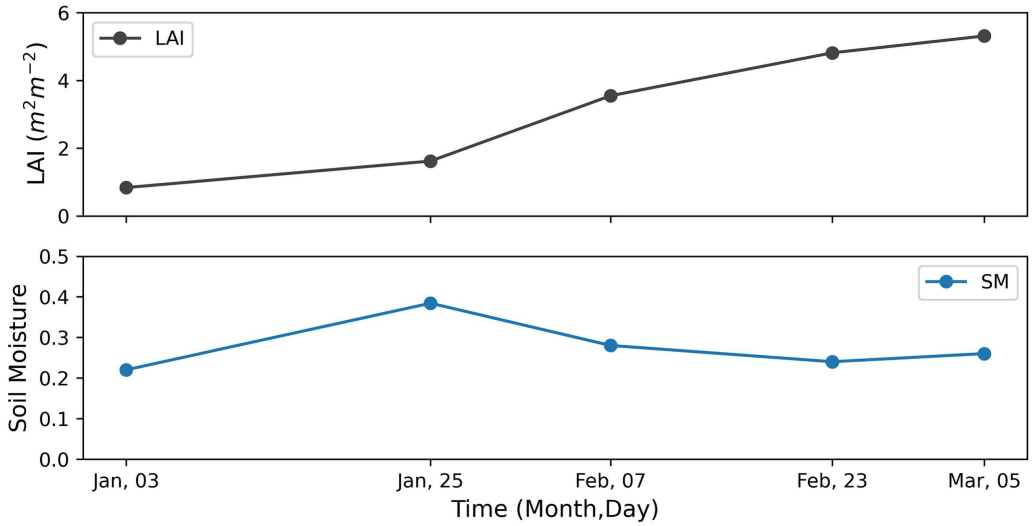

Figure 4.3 Temporal variation of ground measured LAI and soil moisture from January to March 2020.

4.2.3 Satellite data

The Copernicus Sentinel-1 level-1 data products were generated as Single Look Complex (SLC) and employed in mWCM to maximize its capabilities. The datasets of the study region from January to March 2020 were obtained from the Copernicus open-access hub (See Table 4.2.). The Sentinel-1 mission consists of two satellites carrying a C-band SAR imaging device that observed the Earth in four imaging modes (Interferometric Wide, Extra Wide Swath, Strip-Map, Wave). The necessary pre-processing of the Sentinel-1 SLC data was done using the Sentinel Application Platform (SNAP) and its extensions. SNAP is open-source software provided and managed by the European Space Agency (ESA). The complex output of the processed SLC data is used to compute the covariance matrix

(C_2). The 2×2 C_2 is used to calculate the degree of polarization (m), and using the m and backscattering coefficients, the scaling factor for vegetation, soil, and interaction term are derived.

Table 4.2 Characteristics of Sentinel-1 SLC datasets used in the study.

Property of SAR Image	Details
Date of Data Acquisition	02/01/2020, 26/01/2020, 07/02/2020 23/02/2020, 06/03/2020
Polarization	Dual (VV/VH)
Product Type	Level-1, Single look complex (SLC)
Imaging frequency	C-band (5.4 GHz)
Temporal resolution	06 days
Spatial Resolution	10 m
Imaging Mode	IW

4.3 Methodology

4.3.1 SAR data processing

Sentinel-1 data is freely available in two types: Ground Range Detected (GRDH) and SLC from the Copernicus data distribution portal. In this research, SLC data was used to generate the radar backscattering coefficient (σ^0) and a 2×2 covariance matrix. Covariance matrix formulation was done by the terrain-corrected dual-polarized scattering matrix. For the dual-polarized data, the target vector (Equation) is derived from the scattering matrix as

$$\mathbf{k_T} = \begin{bmatrix} S_{VV} \\ S_{HH} \end{bmatrix} \tag{4.1}$$

The 2×2 covariance matrix is derived from the target vector as, $\langle C \rangle = \langle k_T * k_T^{\dagger} \rangle$

$$\langle \mathbf{C} \rangle = \begin{bmatrix} C_{11} & C_{12} \\ C_{21} & C_{22} \end{bmatrix} \tag{4.2}$$

$$\langle \mathbf{C} \rangle = \begin{bmatrix} \langle |S_{VV}|^2 \rangle & \langle S_{VV} S_{VH}^* \rangle \\ \langle S_{VH} S_{VV}^* \rangle & \langle |S_{VH}|^2 \rangle \end{bmatrix} \tag{4.3}$$

$'\dagger'$ represents the Hermitian operator, and '$*$' means the complex conjugate. C is a covariance matrix, representing the spatial average.

4.3.2 Estimation of vegetation, soil, and interaction scaling constant parameter

The ratio of each component of the polarized electromagnetic wave to the total incoming energy is known as the degree of polarization (m). Chang (Chang et al., 2018) assumed the vegetation canopy as a depolarizing media and calculated the m. Subsequently, m is calculated by subtracting one from m, i.e., $1 - m$. Therefore, considering the assumptions made by Chang (Chang et al., 2018), it can be said that the degree of depolarization is directly related to the vegetation canopy. The m is obtained from the covariance matrix. In his investigation, Barakat (Barakat, 1977) determined the formulation of m for the $N \times N$ covariance matrix. In this investigation, the covariance matrix is 2×2, consequently, the expression for m takes the for m as

$$m = \sqrt{1 - \frac{4|C|}{(Trace(C))^2}} \tag{4.4}$$

where C is a 2×2 covariance matrix, depending upon the structure of the vegetation, many radar vegetation indices have been derived, such as RVI, DpRVI, and PRVI, for full and dual-polarized polarimetric data. These indices use vegetation as a depolarizing media and use the degree of depolarization in their formulation. Studies have shown that cross-polarization backscattering coefficients are more sensitive to volume scattering, and quad polarization and dual-polarized bands correlate well (Chang et al., 2018; Holah et al., 2005). In light of these results, we propose a new methodology for vegetation, and soil surface modeling that utilizes Sentinel-1C-band dual-polarized datasets to derive new scaling factors for vegetation, soil, and intermediate layers. The backscattering coefficients and degree of polarization values serve as the basis for the scaling factors, which are crucial in modifying the model so that the output more closely reflects the values actually observed. The scaling factors are determined by using the probability-based scaling approach in which the ratio of backscatter intensities are used to calculate the likelihood of backscattering in the appropriate medial layer. This probability value together with the m is then utilized to scale the model's output, improving the estimate's accuracy and dependability. The inclusion of these extra scaling variables in the mWCM will make it more suitable for local conditions and enable more accurate vegetation and soil surface modeling. The proposed scaling parameters are

$$f_{veg} = \frac{(1-m) * \sigma^0_{VH}}{\sigma^0_{VV} + \sigma^0_{VH}} \tag{4.5}$$

$$f_{soil} = \frac{m * \sigma^0_{VV}}{\sigma^0_{VV} + \sigma^0_{VH}} \tag{4.6}$$

where f_{veg} and f_{veg} parameters correspond to scattering from the vegetation and bare soil surface, respectively. The calculation of the f_{inter} factor can be approached through the following possibilities:

The interaction scaling factor f_{inter}, which describes the interaction between the vegetation and soil surface, can be calculated by different methods. In which some primary ways are, Multiple linear regression (MLR), inversion techniques, and basic mathematical formulae such as $1-(f_{veg}+f_{soil})$ or $f_{inter}=1-f_{veg}*f_{soil}$. Each technique has its own benefits and limitations, and the method employed may be determined by the unique features of the research location and sensor orientation, as well as assumptions made regarding the scattering processes of vegetation and soil surfaces.

Multiple linear regression (MLR) is one of the techniques that can be used to estimate the f_{inter} factor as the dependent variable using various independent variables such as f_{veg}, f_{soil} and other factors. This method allows the consideration of multiple factors that may affect the total backscattering values, but it requires a large dataset which can be computationally expensive.

Inversion techniques may produce a more accurate estimate of the f_{inter} scaling factor. However, this strategy can be difficult and computationally costly and require an independent large dataset.

It is important to note, however, that using the formula $f_{inter}=1-f_{veg}*f_{soil}$ may not be a good idea because it lacks a clear physical interpretation. This is due to the fact that the multiplication of two components does not reflect a quantity conservation, and hence might result in a quantity that is larger than 1, which is not physically conceivable.

Finally, the mathematical formula derived as Equation 4.7 is a simple and straightforward technique to determine the f_{inter}, since it only depends on the values of f_{veg} and f_{soil}.

$$f_{inter}=1-(f_{veg}+f_{soil}) \tag{4.7}$$

By plotting the two formulations $f_{inter}=1-(f_{veg}+f_{soil})$ and $f_{inter}=1-f_{veg}*f_{soil}$ in Figure 4.4 and analyzing the results, it is been observed that the second form of the f_{inter}

equation ($f_{inter} = 1 - f_{veg} * f_{soil}$) exhibits lower values than f_{veg}, which is inconsistent with the expected behavior. This discrepancy suggests that the second form of the equation

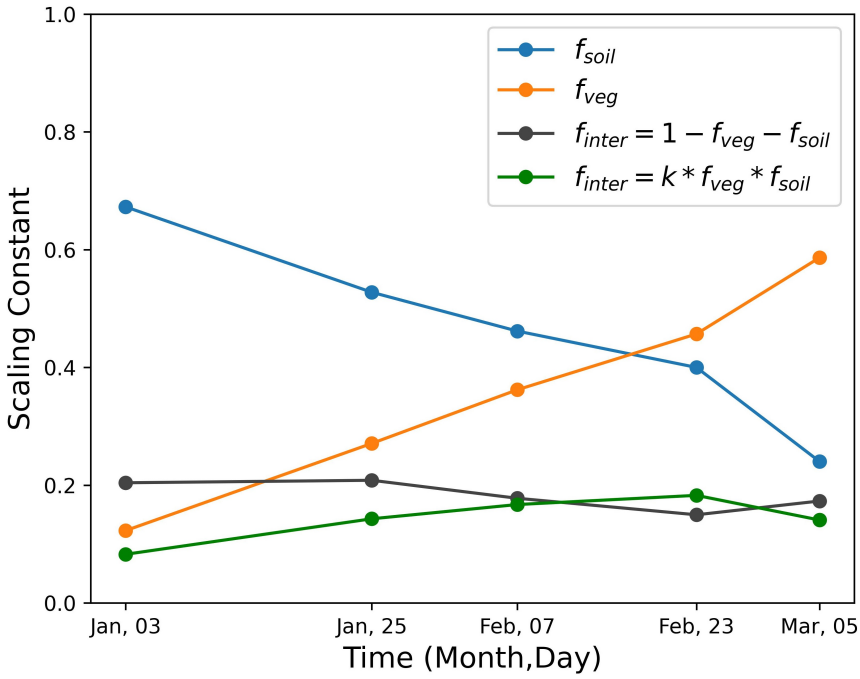

Figure 4.4 The variation of scaling constant f_{veg}, f_{soil} and f_{inter} shown against the time.

may not accurately represent the vegetation-soil interaction. On the other hand, the first form of the f_{inter} equation $f_{inter} = 1 - f_{veg} * f_{soil}$ is more practical and aligns better with the expected behavior. When utilizing the first form, the f_{inter} values are consistent with the vegetation values and provide a more accurate representation of the vegetation-soil interaction. It should be noted that in this analysis, we have taken k = 1 for the second form of the equation f_{inter}. However, the results in Figure 4.4 indicate that any value less than 1 would further decrease the second form of f_{inter}, reinforcing the inconsistency observed.

The plot (Figure 4.4) shows the increasing and decreasing behavior of the backscattering, respectively, for vegetation and soil surface over time with a constant contribution of the interaction term. The interaction contribution is consistent with the proposed third contribution in the WCM described in Section 3.3.

4.4 Modified WCM model

This study uses a semi-empirical WCM to simulate radar-backscattered signals using vegetation and soil parameters. WCM considers the vegetation media as a uniform cluster of spherical-shaped identical bodies homogeneously distributed all over the vegetation layer. The total backscattering coefficient, σ_T^0 for a given set of polarization pq (where pq = VV, VH) can be written as the incoherent sum of backscattering from the vegetation layer (σ_{veg}^0), soil surface (σ_{soil}^0) and vegetation-soil scattering (σ_{inter}^0) shown as an interaction term in Equation 4.8. The scattering from the soil surface is attenuated by the vegetation layer and a two-way attenuation factor (τ^2) is used with the σ_{soil}^0 and σ_{inter}^0 which is defined as

$$\sigma_{pq}^0 = \sigma_{veg,pq}^0 + \tau^2 \sigma_{inter,pq}^0 + \tau^2 \sigma_{soil,pq}^0 \tag{4.8}$$

$$\sigma_{veg,pq}^0 = A_{pq} V_1^{E_{pq}} cos\theta \left[1 - e^{-\frac{2B_{pq}V_2}{cos\theta}}\right] \tag{4.9}$$

Introducing the vegetation scaling constant f_{veg} in the Equation 4.9 to make the modification

$$\sigma_{veg,pq}^0 = f_{veg} * A_{pq} V_1^{E_{pq}} cos\theta \left[1 - e^{-\frac{2B_{pq}V_2}{cos\theta}}\right] \tag{4.10}$$

$$\tau_{pq}^2 = e^{-\frac{2B_{pq}V_2}{cos\theta}} \tag{4.11}$$

where A, B, and E are model parameters that depend upon the canopy type, and polarization channel. θ is radar incidence angle, V_1 and V_2 are vegetation descriptors. In this study, LAI is used as a vegetation descriptor.

For $V_1 = V_2 = V$ backscattering from the vegetation, the Equation 4.12 can be written as

$$\sigma^0_{veg,pq} = f_{veg} * A_{pq} V^{E_{pq}} cos\theta \left[1 - e^{-\frac{2B_{pq}V}{cos\theta}}\right] \tag{4.12}$$

4.4.1 Modified surface scattering Oh model

Oh (2004) provided a semi-empirical model for the bare surface in the form of cross-polarization ratio $\left(\frac{\sigma^0_{VH}}{\sigma^0_{VH}}\right)$ where σ^0_{VH} and σ^0_{VV} refers to VH-polarized backscattering coefficient and VV-polarized backscattering coefficient respectively. The input variables to the semi-empirical model are soil moisture (M_v), incident angle (θ), wavenumber ($2\pi/\lambda$), and surface roughness parameters s and l, where s refers to Root Mean Square Height (RMS) and l to correlation length. A modification in the model was introduced by the implementation of soil scaling constant f_{soil} as

$$\sigma^0_{VH} = f_{soil} * 0.11 M^0_v .7 (cos\theta)^{2.2} \left[1 - e^{(-0.32(ks)^{1.8})}\right] \tag{4.13}$$

$$\frac{\sigma^0_{VH}}{\sigma^0_{VV}} = 0.1 \left(\frac{s}{l} + sin1.3\theta\right)^{1.2} * \left(1 - e^{(-0.9(ks)^{0.8})}\right) \tag{4.14}$$

By substituting Equation 4.13 into Equation 4.14, the backscattering coefficient at VV-polarization can be calculated as

$$\sigma^0_{VV} = \frac{f_{soil} * 0.11 M^0_v .7 (cos\theta)^{2.2} \left[1 - e^{(-0.32(ks)^{1.8})}\right]}{0.1 \left(\frac{s}{l} + sin1.3\theta\right)^{1.2} * \left[1 - e^{(-0.9(ks)^{0.8})}\right]} \tag{4.15}$$

4.5 Vegetation-soil scattering model (VSSM)

In this study, we propose a new backscattering coefficient σ_{inter}. In traditional WCM, backscattering from vegetation and soil surface was assumed, and the interaction scattering between the vegetation layer and soil layer was ignored. In the following derivation, the first order of vegetation scattering and Oh (2004) soil surface model was used to develop the vegetation-soil surface scattering model (VSSM). Figure 4.5 illustrates the backscattering from the vegetation, soil, and interaction phenomenon of vegetation-soil surface.

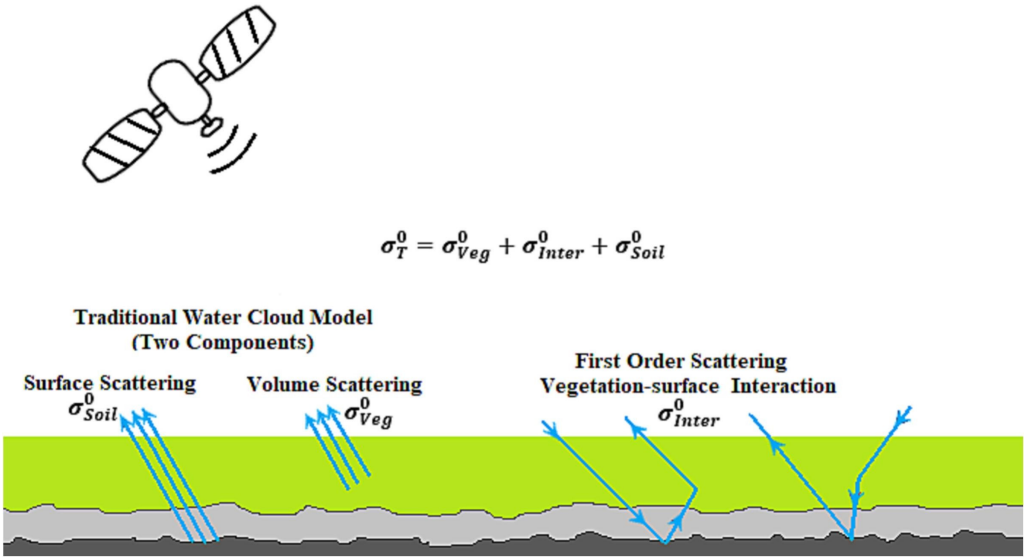

Figure 4.5 Incorporating the vegetation- soil layer interaction scattering component in the traditional WCM.

Equation. 4.9 and 4.13 are adopted in their original form and are expanded according to the Taylor expansion rule to derive the vegetation-soil surface backscattering contribution. After neglecting the higher order terms, the new form of the vegetation backscattering ($\sigma^1_{veg,VH}$) (Equation 4.16) and soil backscattering ($\sigma^1_{soil,VH}$) (Eq. 17) are

$$\sigma^1_{veg,VH} = A_{VH}V^{E_{VH}}cos\theta\left[1-\left(1-\frac{2BV}{cos\theta}+\ldots\right)\right] = 2A_{VH}B_{VH}V^{E^{VH}+1} \tag{4.16}$$

$$\sigma^1_{soil,VH} = 0.11 M_v^{0.7} (cos\theta)^{2.2} \left[1 - \left(1 - 0.32(ks)^{1.8} + \ldots\right)\right]$$

$$\sigma^1_{soil,VH} = 0.11 M_v^{0.7} (cos\theta)^{2.2} * 0.32(ks)^{1.8} \tag{4.17}$$

Multiplication of Equation. 4.16 with 4.17 gives the vegetation-soil surface interaction term or first-order scattering term

$$\sigma^0_{inter,VH} = 0.0704 * A_{VH} B_{VH} V^{E_{VH}+1} M_v^{0.7} (cos\theta)^{2.2} (ks)^{1.8} \tag{4.18}$$

Introducing the vegetation-soil scaling constant (interaction term) f_{inter} in Equation 4.18. Parameters A_{VH} and B_{VH} can be rewritten as $A_{VH}B_{VH} = C_{VH}$ and are polarization-dependent. Thus, the backscattering coefficient of vegetation-soil interaction at VH-polarization will be expressed as

$$\sigma^0_{inter,VH} = 0.0704 * C_{VH} V^{E_{VH}+1} M_v^{0.7} (cos\theta)^{2.2} (ks)^{1.8} \tag{4.19}$$

The interaction term between vegetation and soil at VV-polarization, from Equation 4.14

$$\frac{\sigma^0_{VH}}{\sigma^0_{VV}} = 0.1 \left(\frac{s}{l} + sin1.3\theta\right)^{1.2} * \left(1 - e^{(-0.9(ks)^{0.8})}\right)$$

$$\frac{\sigma^0_{VH}}{\sigma^0_{VV}} = 0.1 \left(\frac{s}{l} + sin1.3\theta\right)^{1.2} * \left(1 - (1 - 0.9(ks)^{0.8} + 0.81(ks)^{0.64} - \ldots)\right)$$

ignoring higher-order terms

$$\frac{\sigma^0_{VH}}{\sigma^0_{VV}} = 0.09 \left(\frac{s}{l} + sin1.3\theta\right)^{1.2} * (ks)^{0.8}$$

by substituting Equation 4.19 in above expression

$$\sigma^0_{inter,VV} = \frac{f_{inter} * 0.0704 C_{VV} V^{E_{VV}+1} M_v^{0.7} (cos\theta)^{2.2} ks}{0.09 \left(\frac{s}{l} + sin1.3\theta\right)^{1.2}} \tag{4.20}$$

Equation 4.19 and 4.20 represent the proposed backscattering coefficients for cross and co-polarized electromagnetic radiation. A new parameter, C_{pq}, has been introduced in these equations, which will require the necessary optimization.

4.5.1 Parametrization and calibration of WCM

The parameterization of WCM is carried out utilizing 70% of the data (training dataset) gathered from three distinct reference fields. The process is attained by an iterative optimization algorithm, such as the Levenberg-Marquardt algorithm, which is used to find the appropriate values of the model parameters which minimizes the sum of squares of the difference between the observed data and the model's predictions. An initial guess for the parameter values is made at the start and then refined through a series of iterations. During each iteration, the simulated values are compared to the observed data, and the parameters are adjusted accordingly to minimize the difference between the two. The algorithm terminates when one of these conditions is met; a maximum number of iterations (e.g., 400), the tolerance level, or the objective function gradient gets sufficiently low (10^{-6}) indicating it has reached a local minimum and additional iteration would not affect the answer (Hosseini et al., 2015). The estimated model parameters were then used to simulate the WCM components and calculate the total backscattering coefficient (σ^0_{total}) using inputs such as scaling factors, soil moisture, and surface roughness. The trained model was then validated on an independent 30% dataset to ensure its unbiased performance in the forthcoming result section. After the parameterization of the model look-up table (LUT) search approach for the inversion of mWCM is adopted (McNairn et al., 2012).

The LUT inversion algorithm was established in MATLAB for the estimation of LAI. The LUT inversion approach facilitated the efficient and rapid estimation of LAI from SAR backscattering coefficients, soil moisture, and scaling constant values.

$$\text{Cost function}(CF) = \sum_{i=1}^{n} \left(\sigma^0_{sim(i)} - \sigma^0_{obs(i)} \right)^2 \tag{4.21}$$

Where σ^0_{obs} is backscattering coefficients computed from Sentinel-1 SAR and σ^0_{sim} is simulated from the mWCM.The model parameters of traditional WCM and mWCM are presented in Table 4.3 and 4.4.

Table 4.3 The details of the model parameters optimized in the WCM.

Polarization	**A**	**E**	**B**
VV	0.051	1.271	0.663
VH	0.054	1.211	0.721

Table 4.4 The details of the model parameters optimized in the mWCM.

Polarization	**A**	**E**	**B**	**C**
VV	0.085	1.102	0.583	0.0495
VH	0.081	1.170	0.637	0.0520

4.6 The sensitivity analysis of the proposed mWCM

The Figures 4.6 and 4.7 show the sensitivity analysis of the mWCM against the LAI and different soil moisture values respectively. The soil moisture values in our observation varied from 0.1 $m^3m^{-3}$to 0.4m^3m^{-3}. Therefore, we generated sensitivity analysis for three soil moisture values 0.1m^3m^{3-}, 0.25m^3m^{-3}, and 0.38m^3m^{-3}. The analysis is presented for VH and VV polarizations in Figs. 6 and 7 respectively. In both VV and VH polariza-

tions, vegetation attenuated backscattering values for soil surface and interaction ($\tau^2\sigma^0_{soil}$, $\tau^2\sigma^0_{inter}$) are plotted so that variations in each component can be visualized easily.

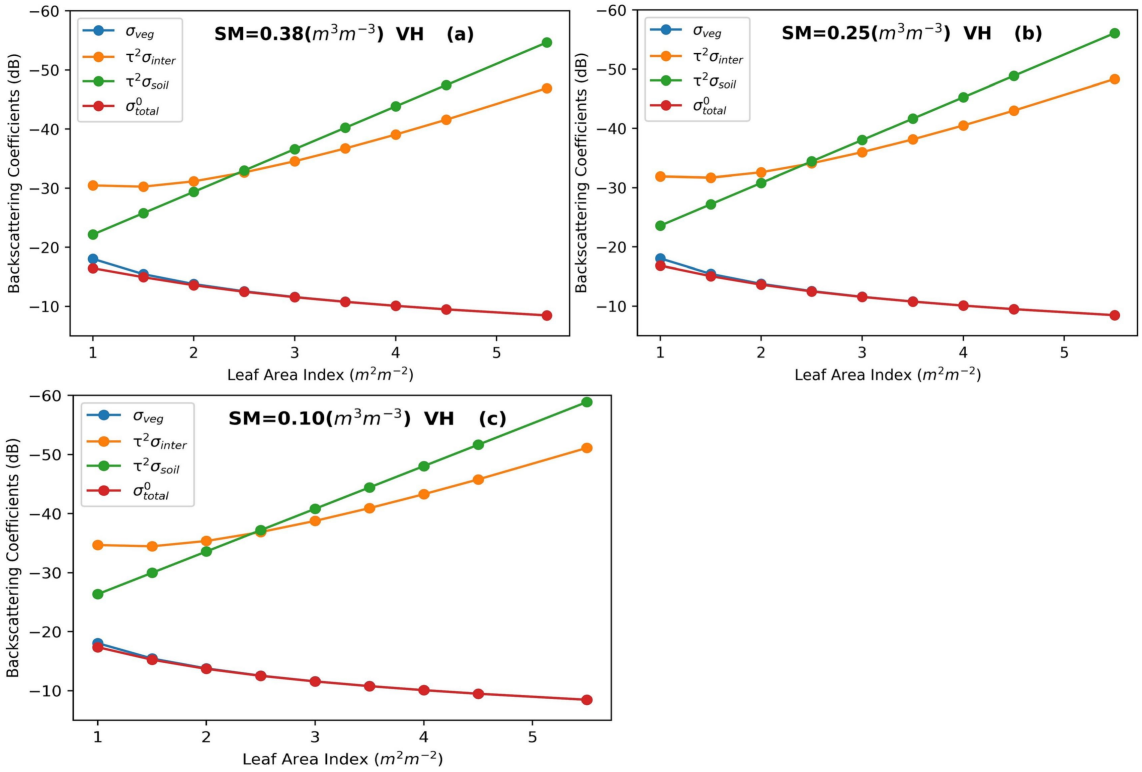

Figure 4.6 Behavior of σ^0_{veg}(blue), $\tau^2\sigma^0_{soil}$(green) and $\tau^2\sigma^0_{inter}$(orange) at VH polarization against LAI with different values of soil moisture (SM), (a) 0.38, (b) 0.25, (c) 0.10 keeping surface roughness (s) and correlation length (l) constant.

In Figure 4.6, for VH polarization, the soil moisture value decreases (graph a to c) backscattering contribution from the soil surface (green) and interaction (orange) to the total backscattering value (red). This suggests that as the soil moisture decreases the backscattering from the bare surface also decreases. The attenuated interaction backscattering when the LAI value is lower or when the crop is in its early days, the attenuated interaction backscattering ($\tau^2\sigma^0_{inter}$) contributes less than the attenuated soil backscattering however as the LAI value increases, the backscattering from attenuated interaction is overtaking the soil surface contribution. Since, the σ^0_{veg} (blue) is proportional to LAI

(Equation 4.12) therefore its, contribution is found dominant among all the components contributing to mWCM.

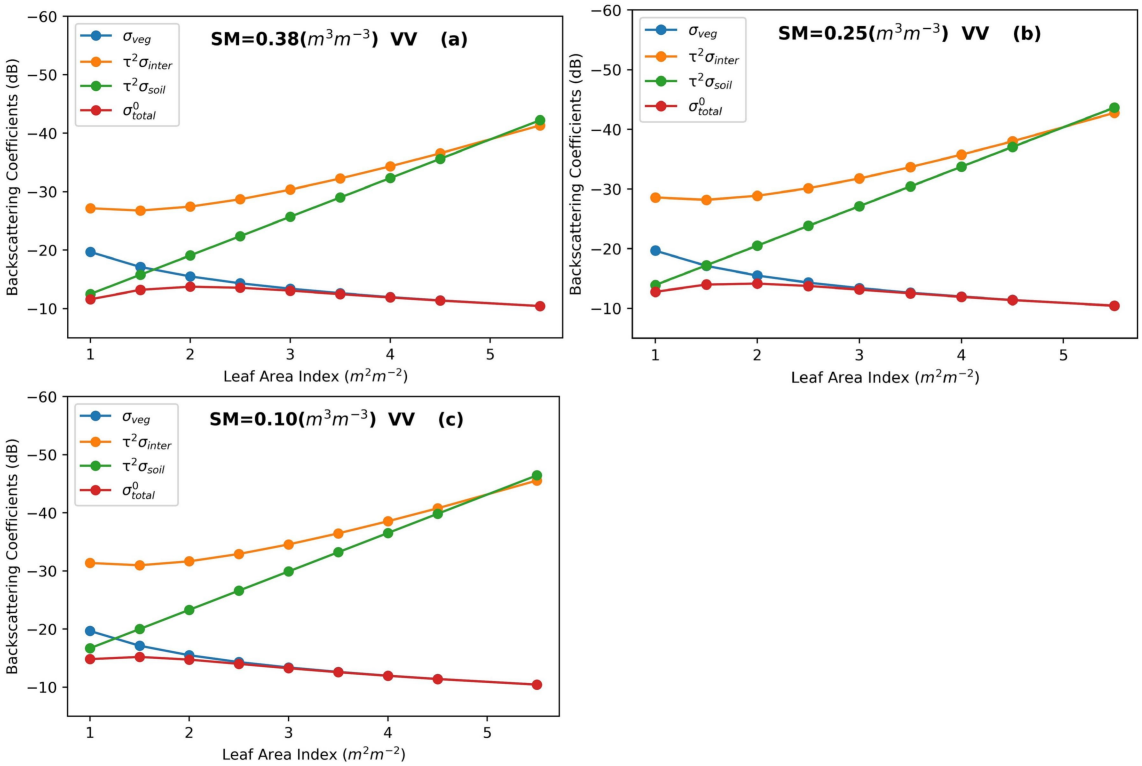

Figure 4.7 Behavior of σ^0_{veg}(blue), $\tau^2\sigma^0_{soil}$(green) and $\tau^2\sigma^0_{inter}$(orange) at VV polarization against LAI with different values of soil moisture (SM), (a) 0.38, (b) 0.25, (c) 0.10keeping surface roughness (s) and correlation length (l) constant.

For VV in Figure 4.7 polarization, the sensitivity analysis is showing a different behavior than the VH polarization. At lower values of LAI, the backscattering contribution of the soil surface is more than the vegetation and interaction backscattering. As the LAI is increasing the contribution from the vegetation is again increasing and soil surface and interaction contribution to the total backscattering started to decrease. In this sensitivity analysis, it is clearly shown that as the soil moisture decreases the soil surface contribution decreases whereas the modification term in the WCM starts to make a significant contribution when the LAI is about 2 for VH polarization. It is worth noting that VV polarization

is more sensitive to the vegetation and soil properties whereas the variation in vegetation features is more prevalent in the VH polarization.

4.7 Results

4.7.1 Investigation of relation between vegetation and m

Figure 4.8 shows the manifesting change on land from January to March 2020. The graph with five points represents the five days for data collection, and each point represents the average value of the m of the day. Each pixel in the colored maps represents the m of the study site over the vicinity of the Ganga River derived from the C_2 matrix of SLC datasets. The general impression of Figure 4.8 indicates that the average value of the m decreases as

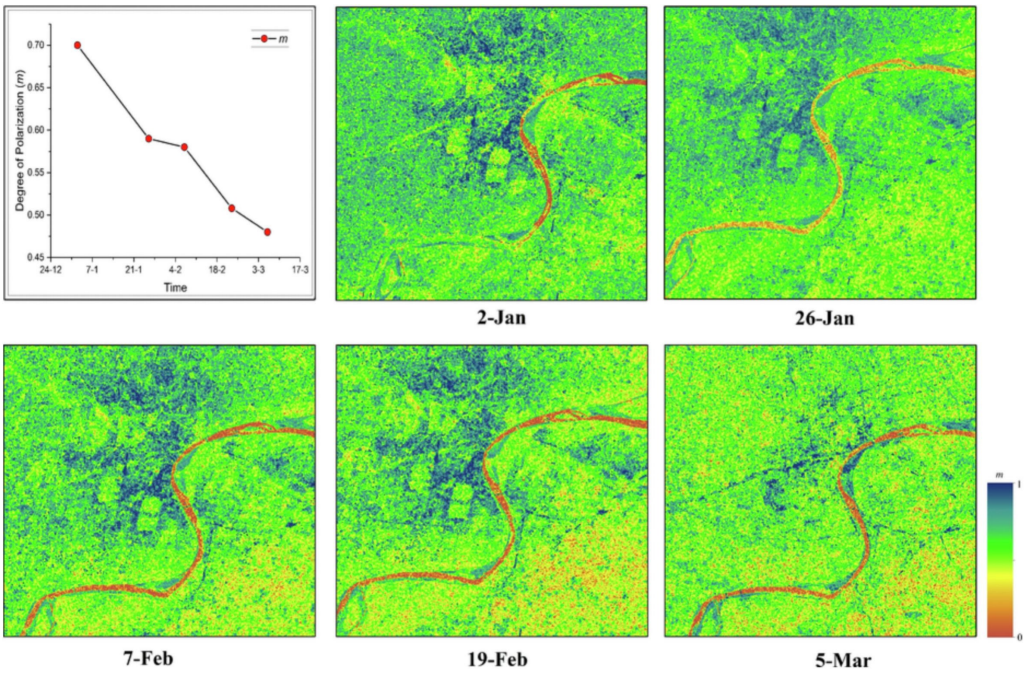

Figure 4.8 The variation of m from January to March 2020. The graphical presentation (upper left) of the m shows that its value decreases as the crop gets denser. The following images are time-series satellite images that illustrate the m's declining value.

the vegetation increases. Several studies have related the change in m with the change in vegetation cover (Chang et al., 2018; Mandal et al., 2020). As the vegetation increases,

it acts as a depolarizing medium to the incoming polarized electromagnetic radiation. After interacting with the vegetation, the electromagnetic radiation gets depolarized, and consequently, the coefficients m decrease. This change was apparent in the result; the blue color in maps represents the high intensity of *m*, and as the blue gets transitioned towards the yellow value, the measuring quantity *m* decreases. In the early days of crop growth, the vegetation, and its density are less, so the coefficient *m* has a higher value throughout the region, but as the crop gets bigger and bigger and foliage increases, the color of the maps shifts towards yellow, bolstering the assumption that vegetation act as a depolarizing media for the polarized electromagnetic energy.

4.7.2 Calculation of backscattering coefficient and WCM inversion

The WCM in its original simplified form using the soil scattering model has been tested by several studies (Baghdadi et al., 2017). The SAR backscattering phenomenon was not independent; it depended on vegetation properties such as plant height, density, and structure. Therefore, the different vegetation types can produce different calibration behaviors and parameters. In this part of the study, the traditional version of WCM was validated on an independent 30% dataset to ensure its unbiased performance. Past studies (Holah et al., 2005; Li et al., 2014) have suggested that VV and cross-polarization (VH) were more sensitive to surface and vegetation properties, respectively. The WCM was parametrized for both of the polarizations. Table 4.3 contains the calibrated WCM parameters A, B, and E obtained from the observed vegetation descriptor (LAI) following the training procedure. The performance of the calibrated model was evaluated by comparing the SAR backscattering coefficient and estimated backscattering coefficient values. Figure 4.9 shows the scatter plot between observed backscattering (σ^0_{obs}) on the x-axis and estimated backscattering (σ^0_{est}) on the y-axis. The comparison was performed for VV and VH polarization on a 1:1 line as a reference. For VV polarization, the estimated and observed backscattering

coefficients were less correlated (R^2 = 0.77, NSE = 0.74) than the VH polarization (R^2 = 0.80, NSE = 0.76). The result suggests that at VH polarization model was better calibrated than the VV. In addition, the errors associated with VH polarization (RMSE = 0.68 $m2m^{-2}$) were also lower than the result at VV polarization (RMSE = 0.70 $m2m^{-2}$). The trained

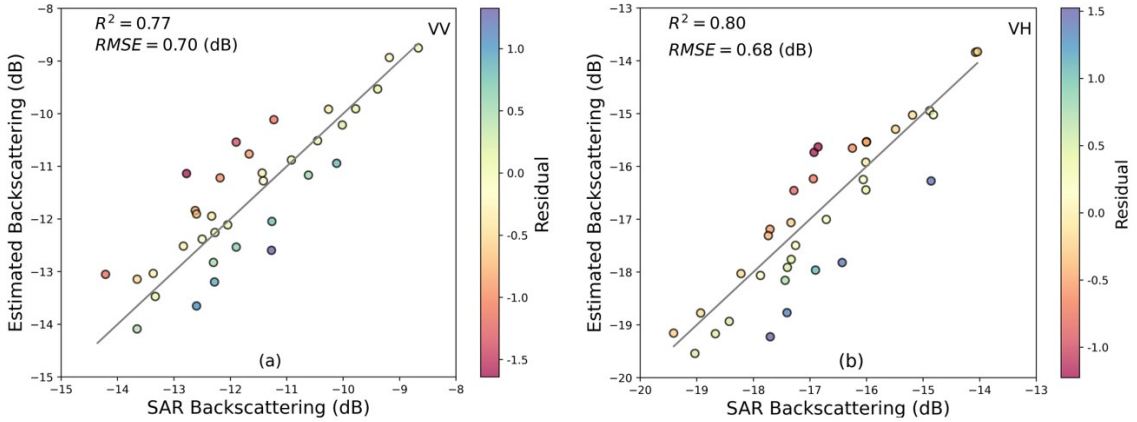

Figure 4.9 Estimated backscattering coefficient (a) For VV polarization, (b) For VH polarization against SAR backscattering coefficient.

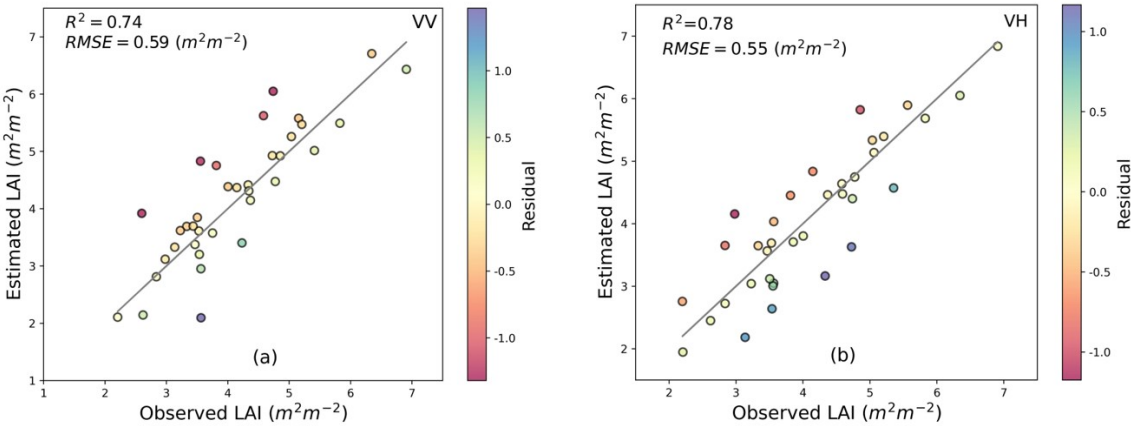

Figure 4.10 Estimated LAI from model inversion for (a) VV polarization, (b) VH polarization and validated against in-situ datasets.

WCM comprising the vegetation and soil backscattering effect was further inverted to retrieve the LAI and SM. Figure 4.10 shows the scatterplot between the obtained LAI (from the inversion of calibrated WCM) and the observed LAI. The LAI at VH was more accurately estimated than the VV polarization. It was not surprising because in the forward

modeling VH estimation was better. The evaluation recorded R^2 = 0.74, NSE = 0.72 and RMSE = 0.59 m^2m^{-2} at VV polarization in comparison to better R^2 = 0.78, NSE = 0.75 and lower RMSE = 0.5493 m^2m^{-2} at VH polarization. Figure 4.11 shows the scatterplot between the obtained SM and the estimated SM. In this case, SM at VV polarization has shown better accuracy than the VH polarization. The evaluation recorded R^2 = 0.74, NSE = 0.73 and RMSE = 0.051 m^3m^{-3} at VV polarization in comparison to R^2 = 0.73, NSE = 0.72, and higher RMSE = 0.056 m^3m^{-3} at VH polarization.

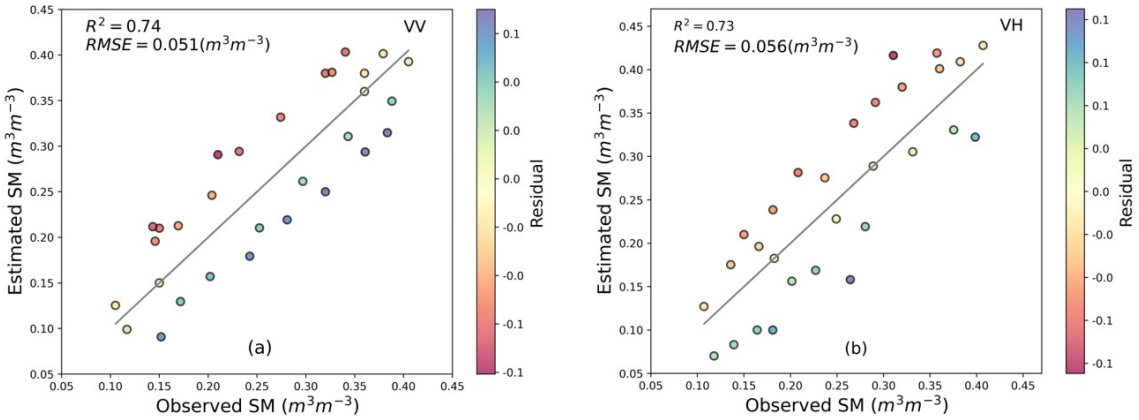

Figure 4.11 Estimated SM from model inversion for (a) VV polarization, (b) VH polarization and validated against in-situ datasets.

4.7.3 Calculation of backscattering coefficients and WCM inversion after including first-order scattering

The WCM, in its simplified form, relates the contribution of vegetation and surface individually by using concerned backscattering coefficients. It does not discuss the contribution arising from the interaction between surface and vegetation. The methodology section explains the derivation and assumption used in deriving the backscattering coefficient applicable to vegetation-surface scattering interaction. The interaction term was polarization-dependent Equation 4.19 and 4.20. The model equation was parametrized using the least square regression, and consequently, model parameters A, B, C, and E

were calculated. Using these model parameters, the model accuracy was tested. The backscattering coefficients at VV and VH polarization were evaluated by means of forward modeling and shown in figure 4.12. The additional interaction term in mWCM improved

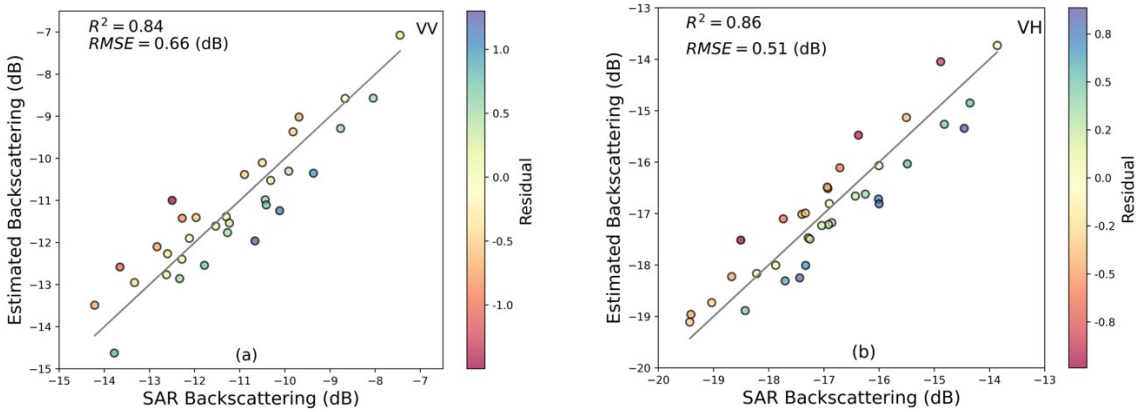

Figure 4.12 Estimated backscattering coefficient for (a) VV polarization and (b) VH polarization against SAR backscattering coefficient.

the accuracy of the backscattering estimation. The VH estimation produced better accuracy with higher R^2 = 0.86, NSE = 0.85 in comparison to the earlier estimation, which was lower (R^2 = 0.80, NSE = 0.76). A similar increase in accuracy was also seen in the VV estimation. The reported R^2 and NSE were 0.84 and 0.84, respectively, in comparison to earlier R^2 = 0.77, NSE = 0.74. The errors associated with these estimations were also improved significantly for VH estimation. It was improved from RMSE = 0.68 m^2m^{-2} to RMSE = 0.51 m^2m^{-2} and for VV estimation it was improved from RMSE = 0.70 m^2m^{-2} to RMSE = 0.66 m^2m^{-2}. The addition of the interaction term clearly improved the results.

The mWCM was inverted to evaluate the model's performance and retrieve the LAI and SM. As the results of the backscattering coefficients at both the polarization improved significantly. Similar behavior of improvement was also seen in the LAI and SM estimation accuracy shown in Figures 4.13 and 4.14, respectively. The R^2 and NSE values between estimated LAI and observed LAI for VH polarization were 0.80 and 0.78, respectively; for VV polarization, the value was 0.78 and 0.77, respectively. The errors associated with the inversion of mWCM were also lowered. The RMSE between estimated LAI and observed

LAI for VH and VV polarizations were 0.44 m^2m^{-2} and 0.53 m^2m^{-2}. The VH polarization estimated better accuracy in LAI estimation in both cases. The R^2 and NSE values between

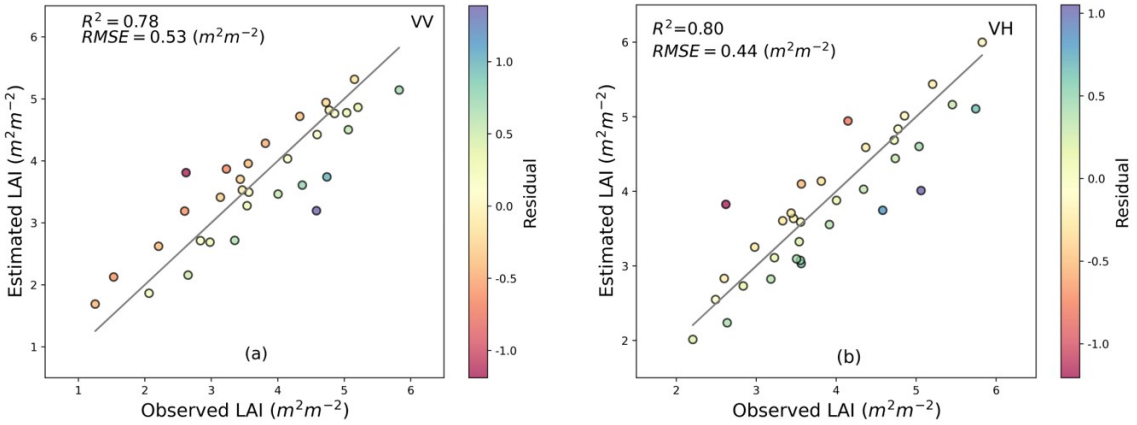

Figure 4.13 Estimated LAI for (a) VV polarization and (b) VH polarization. Against in-situ LAI.

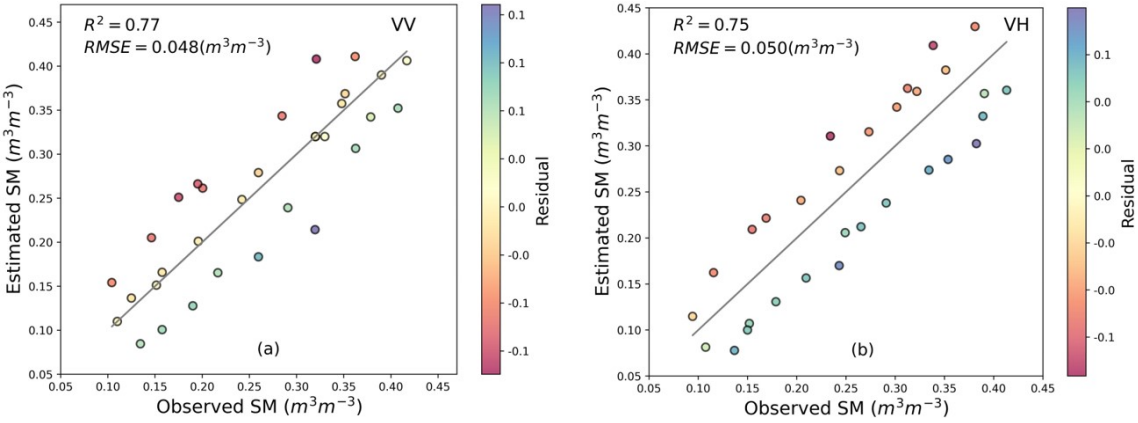

Figure 4.14 . Estimated SM from model inversion for (a) VV polarization, (b) VH polarization and validated against in-situ datasets.

estimated SM and observed SM for VV polarization are 0.77 and 0.79, respectively; for VH polarization, the values are 0.75 and 0.76, respectively. The errors associated with the inversion of mWCM are also lowered. The RMSE between estimated LAI and observed LAI for VV and VH polarizations are 0.048 m^3m^{-3} and 0.050 m^3m^{-3}. Subsequently, a relationship between the retrieved LAI and the SAR backscattering coefficients has been established. This relationship is then applied to the radar data, resulting in the generation

of LAI maps for our study region. The Figure 4.15 shows the spatial-temporal maps of LAI at VV and VH polarizations.

According to the modification proposed in this study, accuracy towards vegetation at VH (cross-polarization) was better than VV polarization. The higher accuracy of cross-polarization is most likely due to the increase in the value of backscattering coefficients at different phenological stages of the wheat crop. In the maps, the upper region of the river is the plane landscape, and below it is partly hilly. The spatial variation of LAI over the upper part of this extensive landscape in Figure 4.15(a) demonstrates that the average value of LAI increases from the early stage of vegetation on January 2, 2020, to its peak on March 5, 2020 map. A similar kind of pattern can also be observed in Figure 4.15, but the estimation accuracy at VH polarization was found more in comparison to VV polarization which is evident in this estimation from visualization.

Figure 4.16 exhibits the spatio-temporal SM maps, portraying the VV and VH polarizations, which are derived utilizing the relationship between the estimated SM and radar data. In Figure 4.16(a), the temporal variation of the SM appears to be relatively constant, indicating minimal fluctuations in soil moisture levels, as observed in the in-situ SM datasets shown in Figure 4.3. However, on 26 Jan 2020, a little increase in the pixel values of SM is seen in the upper part map due to the precipitation at that time. A similar pattern in variation is also seen for the VH case shown in Figure 4.16(b). Moreover, the estimation accuracy is notably superior in the VV estimation for SM compared to the VH polarization (El Hajj et al., 2017; Zribi et al., 2014).

4.8 Conclusion

Remote sensing with the help of satellite data made surface and vegetation mapping very useful and efficient. In this study, the traditional WCM is modified using the surface vegetation interaction term. The calibration of the traditional WCM and mWCM was done

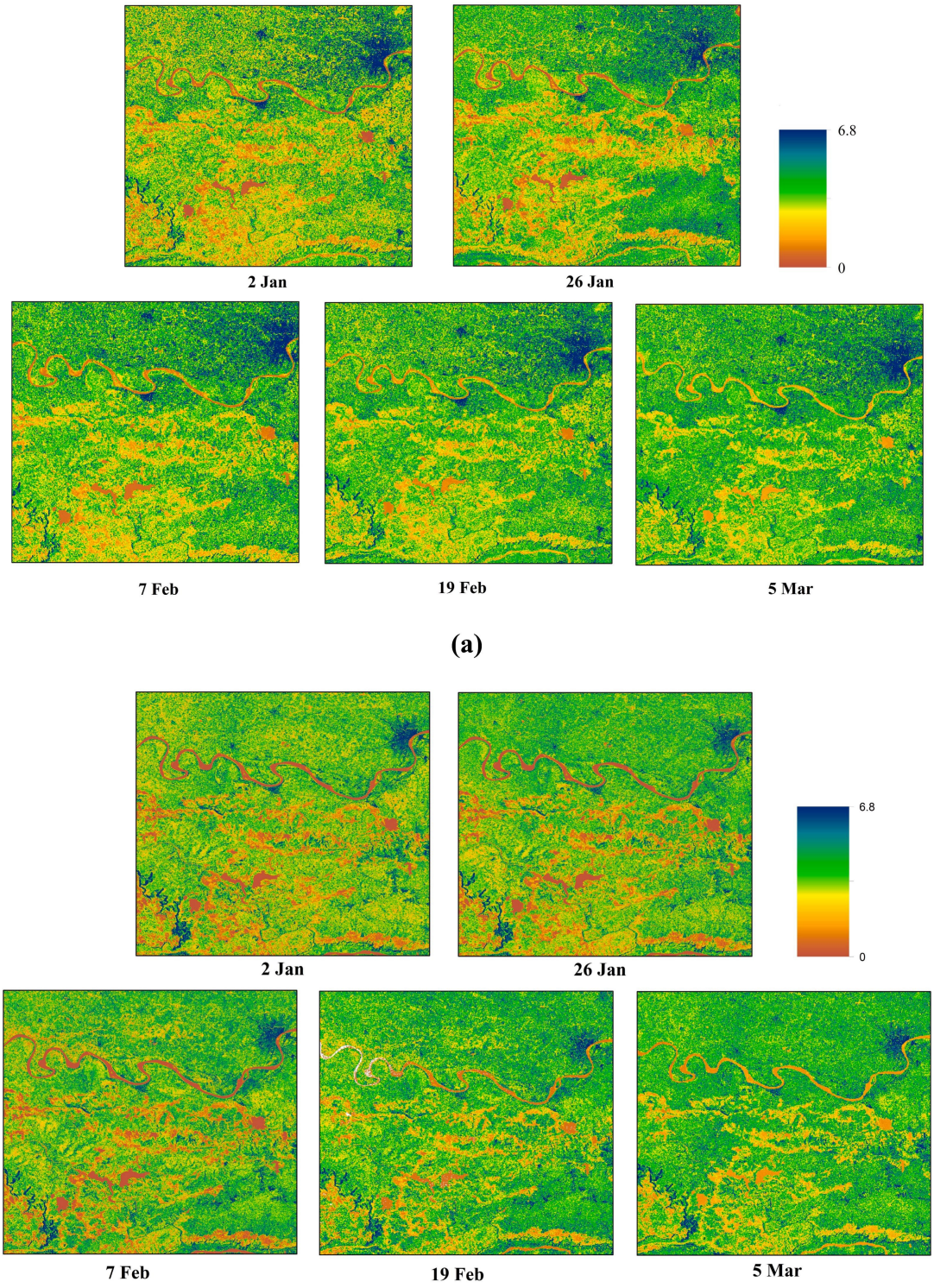

Figure 4.15 The two sets of spatial-temporal maps at (a) VV polarization and (b) VH polarization show the LAI estimation in the large landscape.

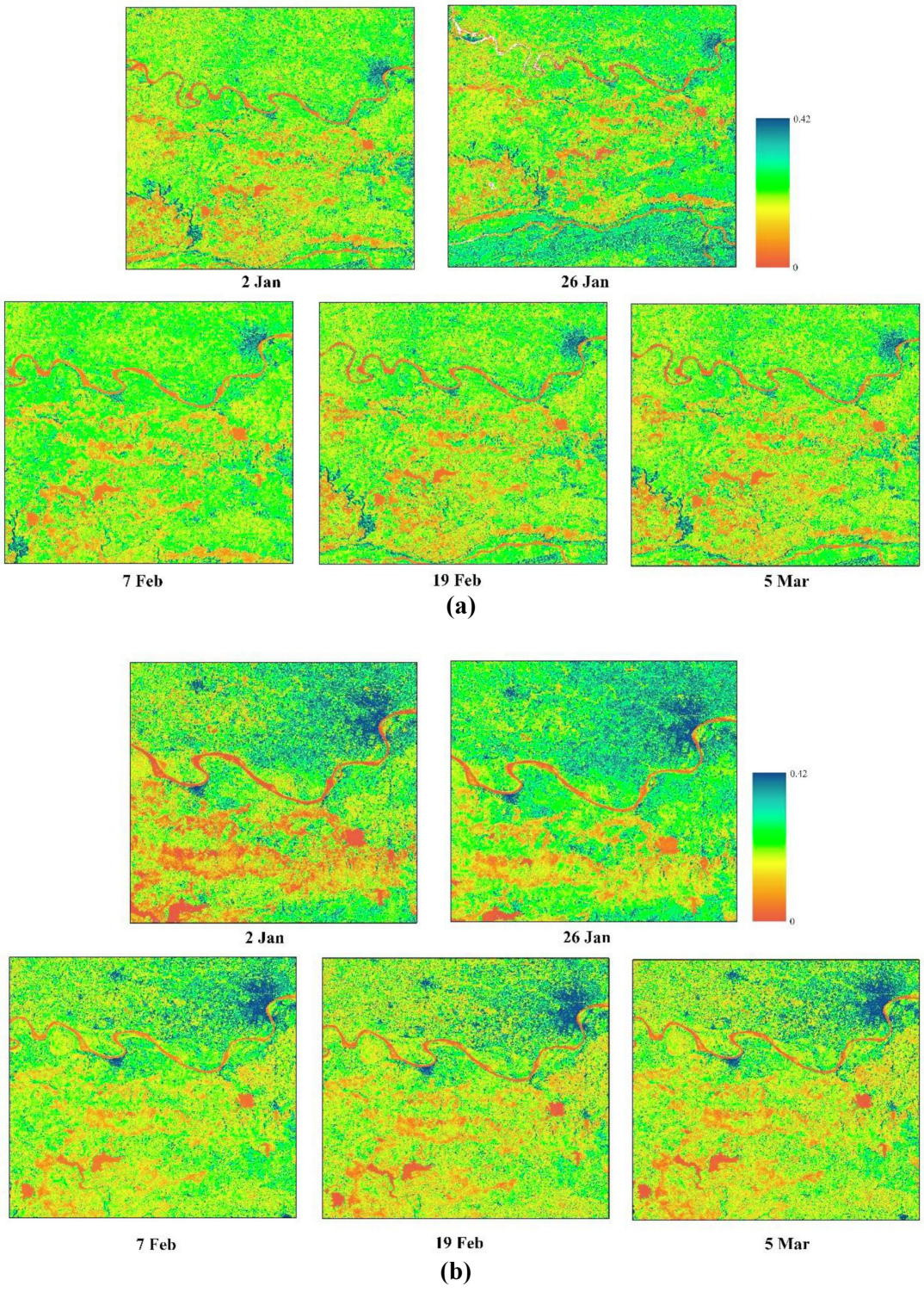

Figure 4.16 The two sets of spatial-temporal maps at (a) VV polarization and (b) VH polarization show the SM estimation in the large landscape.

using the C-band Sentinel-1 SAR data, in-situ measurements of LAI, and soil surface parameters such as soil moisture, and surface roughness over crop fields.Oh (2004) surface model was used in WCM and mWCM to model the effect of soil on the overall radar backscattered signal. The objective of the study was to enhance the accuracy and reliability of the WCM by modified backscattering coefficients through novel scaling constant and incorporating a new vegetation-soil backscattering term.

The results from the mWCM are improved when compared with the simplified WCM. From the sensitivity analysis, it is evident that the magnitude of contribution from the interaction term in total backscattering was less when the LAI was less but it started to contribute significantly enough when the LAI is above 2.0 m^2m^{-2}. The proposed modification in the WCM increased the R^2 between estimated and observed backscattering coefficients σ^0_{VH} and σ^0_{VV} by 7.03% and 8.62%, respectively. For VH and VV polarizations, the R^2 between observed and estimated LAI (after inversion) are also improved and increased by 1.58% and 3.6%, respectively. For SM, a better improvement is seen in VV polarization with a 4.1% increase than the VH with 2.7%. The RMSE between estimated and observed backscattering coefficients and LAI are reduced by 25.25% and 19.4%, but 6.00% and 9.86% for VV polarization, respectively, and for SM, the reduction is 5.88% in VV and 1.1% in the VH polarization. The interesting behavior in the improved accuracy is that the improvement in the R^2 for VV polarization estimations is higher for backscattering coefficients, SM, or LAI than the estimation from the VH polarization. However, reductions in the RMSE for backscattering coefficients and LAI have been observed lower in the VH polarization and for SM it is in VV polarization. The studies have reported that cross-polarization data is more sensitive to the vegetation and co-polarized data is more susceptible to surface properties. However, the proposed algorithm in this research provided the following scientifically significant results:

1) The effective scaling factors (i.e., f_{veg},f_{soil}, f_{inter}) derived from polarimetric SAR data using scattering wave vectors played a vital parameter in mWCM to improve the electromagnetic SAR signal strength backscattered from vegetation, soil surface, and other order backscattered power. As a result, it strengthens the mWCM retrieval capabilities of LAI and SM to address the poorly stated retrieval issues when the vegetation and soil surface have reflectance values that are nearly similar.

2) In the proposed study, the incorporation of first-order backscattered power in terms of $\sigma^0_{inter,pq}$ marked the additional sensitive signal parameter in the homogeneous/ non-homogeneous vegetative areas and the microwave vegetation scattering algorithms to infer the retrieval results. Therefore, the mWCM-based inversion algorithm developed in the present study provided better inversion results than traditional WCM for estimating LAI and SM at VV and VH polarizations.

Based on the findings of this study, it can be concluded that while the VH polarization provided a higher accuracy in the LAI estimation, whereas VV polarization provided a higher accuracy in the SM estimation. Incorporating information from the VV polarization could still be useful in improving the overall accuracy and robustness of the results. A balanced approach would be to use a weighted combination of the estimates from both VV and VH, considering the superior accuracy of the VH estimate for vegetation and VV for soil properties. Therefore, the coupled VH and VV polarization are recommended for vegetation and surface study. Additionally, the study also proposes a modification in the WCM to make it more compatible with the local conditions.